CORRELATION OF THIN-FILM BOND COMPLIANCE AND BOND FRACTURE RESISTANCE

R.C. Addison Jr. and D.B. Marshall

Rockwell International Science Center
Thousand Oaks, CA 91360

ABSTRACT

The integrity of the interfacial bond between a coating and its substrate is of primary importance for any application. A technique for the quantitative nondestructive measurement of the bond fracture energy is essential for evaluating bond integrity. Scanning acoustic microscopy (SAM) provides a method for making localized measurements of film disbonds and film bond compliance based on the changes in the surface acoustic wave velocity in the layered medium. The results of these measurements for chrome/gold and gold films on glass substrates are summarized. The compliance of the bond and its fracture energy can be correlated in some film systems. An experiment to determine if this correlation exists for chrome/gold and gold films on sapphire substrates is described. Results of such an experiment would provide an empirical correlation between surface acoustic wave velocity measurements and the fracture energy of the film. The results of an experiment to measure the fracture energy of the interfacial bond between a gold film and the sapphire substrate are described.

INTRODUCTION

Although the integrity of the interfacial bond between a thin-film and its substrate is the most important property for any application, there are currently no techniques for measuring the fracture energy of the bond that are nondestructive, quantitative, reproducible, and reliable. Several reviews have been published describing the measurement techniques that are available [1-4]. Generally stated, a nondestructive adhesion measurement test must be able to apply a tensile stress to the film bond and detect the response of the bond without causing damage. A convenient way of doing this is to use mechanical energy via an acoustic wave. For detecting the response, some favorable results have been obtained using scanning acoustic microscopy techniques to measure surface acoustic wave velocities [5,6].

In a scanning acoustic microscope, a high numerical aperture acoustic lens is used to focus an acoustic beam on the surface [7,8]. The angles of incidence are sufficiently large to excite surface waves which create stresses at the film substrate interface. Changes in the adhesive bond can lead to changes in the boundary conditions that cause slight changes in the velocity of the surface acoustic waves. The velocity can

be measured by varying the distance between the surface and the acoustic lens. This technique can provide a measure of the compliance of the bond between the film and the substrate. To use such measurements for NDE would require the use of a destructive technique to measure the fracture energy of the bond and then determination of whether a correlation exists between the compliance and fracture energy. A correlation is likely if interfacial failure occurs by brittle fracture as in many thin-film/substrate systems [9]. A simple indentation method for determining the fracture energy of interfaces between thin films and substrates has been developed [9,10]. We have adapted this method to a film system consisting of chrome/gold and gold on a sapphire substrate.

SURFACE ACOUSTIC WAVE (SAW) VELOCITY MEASUREMENTS

Specimens were prepared with films and substrates for which the physical mechanisms producing the adhesive bond were known. Details of the preparation are given elsewhere [6]. Two films, one chrome/gold and the other gold, were deposited on a common substrate of soda lime glass, as shown in Fig. 1. An overcoating of chromium was deposited on both films. This is not expected to affect the adhesive properties of the film.

The data for determining the SAW velocities were acquired in G.A.D. Briggs' laboratory at Oxford University using custom equipment similar to that described by Kushibiki and Chubachi [5]. All specimens tested were prepared according to the same procedure. The chromium base layer film is of negligible thickness as far as the acoustic measurement is concerned. Both the gold film and the chromium overcoat have uniform thickness and composition over the entire specimen. Therefore the only variation in the SAW velocity between the two halves of the specimen should be due to changes in the film adherence. Four specimens were prepared with the labels UCL1, KH2, KH3, and KH4.

An image, shown in Fig. 2, of the boundary between the chromium base layer (CBL) and the gold base layer (GBL) regions of specimen UCL1 was obtained using a scanning acoustic microscope operating at 400 MHz. The contrast mechanism is due to differences between the V(z) response between the two regions. It is not possible to obtain a quantitative estimate of the difference in the SAW velocity from this image, but it clearly shows that the two regions have different responses. The data for all the specimens is summarized in Fig. 3. Here the average of the

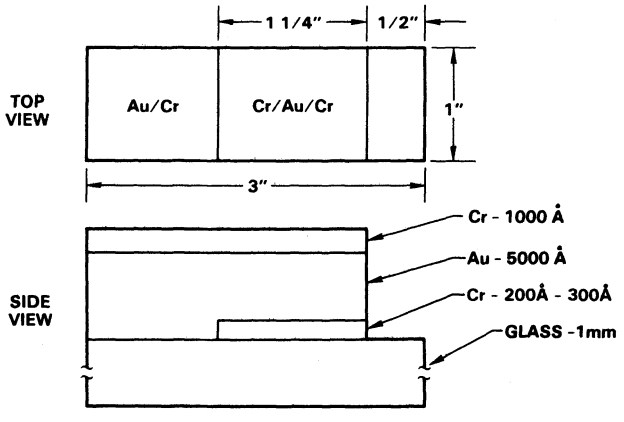

Fig. 1. Schematic showing film layers and thicknesses.

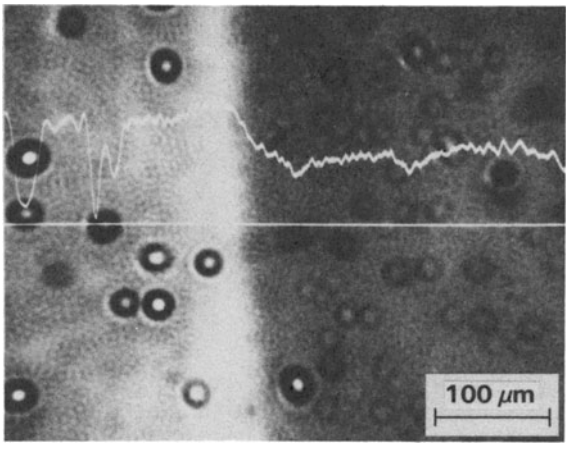

Fig. 2. Scanning acoustic microscope image (400 MHz) of the boundary between the CBL region on the left and the GBL region on the right. Width of image is about 500 μm. (Photo made by M. Hoppe, E. Leitz Instruments Inc.)

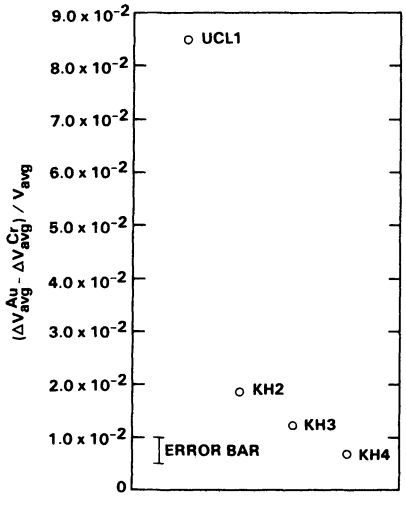

Fig. 3. Summary of four sets of measurements. Note that the SAW velocities in the GBL region are larger than those in the CBL region for all specimens.

velocities in the CBL region of each specimen has been subtracted from the average of the velocities in the GBL region of that specimen and normalized to the overall average velocity in both regions. For all four specimens, the difference has the same sign indicating that there is a clear distinction between the two regions of different film adhesion.

The cause of the SAW velocity shift as the film adherence changes can be attributed to a change in the compliance of the bond between the film and the substrate. To verify that bond compliance changes can produce SAW velocity shifts of this magnitude, it is of interest to calculate the changes in the SAW velocity that occur as the bond compliance

changes. Bray [11] has developed a procedure for calculating the complex reflectivity and hence the leaky SAW velocity for a layered substrate. His model assumes that the layers are in intimate contact with noncompliant bonds between each layer. Thompson and Fiedler [12] have developed a model for a compliant boundary condition that they have used to explain acoustic wave propagation through tightly closed cracks. This boundary condition has also been successfully used by Punjani and Bond [13] in numerical calculations of scattering of plane waves from cracks. This boundary condition assumes that there is a massless spring at the boundary that allows a discontinuity in the velocity across the boundary. The boundary condition can be expressed as

$$\vec{V}^{n+1} - \vec{V}^{n} = \frac{\partial}{\partial t} [\overleftrightarrow{h} : \overleftrightarrow{T} \cdot \vec{n}] \qquad (1)$$

where n is the number of the layer, $\overleftrightarrow{h}$ is the compliance tensor, $\overleftrightarrow{T}$ is the stress tensor, and $\vec{n}$ is a unit vector normal to the film interface in the positive z direction. For this problem, the compliance tensor has only two components corresponding to the compressional compliance and the transverse compliance.

After Bray's model was modified to incorporate the massless spring boundary conditions, results were calculated for the film system used in the experiments. The effects of changes in the compressional compliance on the leaky SAW velocity are plotted in Fig. 4. The curve for changes in the SAW velocity vs changes in the transverse compliance is similar to the one shown in Fig. 4. We assume that the compliance of a good bond, such as that observed in the CBL region, is much less than 10^{-16} cm^3/dynes. Thus the change in the SAW velocity observed in the data (Fig. 3) can be compared to that of a bond of zero compliance. Note that it is possible to obtain changes in the SAW velocity that are even greater than the ones observed in the experiments. Further, in the range of SAW velocity shifts observed in the experiments, the change in the SAW

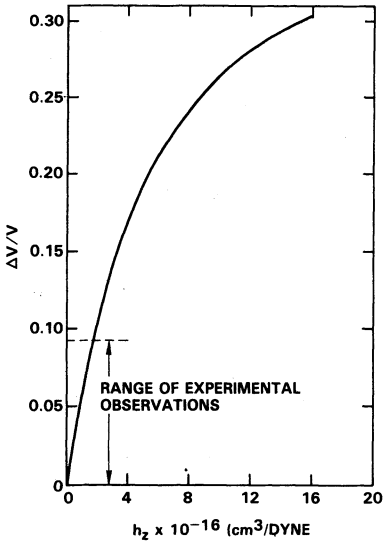

Fig. 4. Change in leaky SAW velocity vs the compressional compliance, h_z, of the bond between the film and the substrate. The transverse compliance, h_x, is zero.

velocity is a linear function of the compliance. This result suggests that changes in the SAW velocity can be a direct measure of changes in the compliance of the bond between the film and the substrate.

INDENTATION MEASUREMENTS

Indentation measurements were made with a different set of specimens than those used for the acoustic measurements. After acquiring and analyzing the acoustic data there was concern that the variability of the mechanical properties of the poorly characterized soda-lime glass might produce an unwanted variation in the measurements. Therefore for the indentation measurements, this possibility was eliminated by changing the substrate to a single crystal sapphire disk with a diameter of 1.0 in. and a thickness of 0.02 in. The chrome/gold and the gold films were deposited on separate substrates with the nominal thickness of the gold film being 5000Å for both specimens. Ultimately it will be desirable to have both the chrome/gold and the gold films on a common substrate, as was done with the acoustic measurements, to minimize variations that might be caused by differences in the film deposition parameters.

Initially we tried loading a Vickers indenter onto the surface of the film to create a disbond between the film and the substrate as was performed previously in a ZnO/Si film/substrate system [10]. The disbond produced by this type of indenter was irregular in shape and variable in size. However, a spherical indenter (400 μm diameter tungsten carbide ball) produced disbonds in the gold/sapphire system that were circular with highly reproducible dimensions that could be clearly seen in Nomarski micrographs. Measurements from optical interference micrographs indicated that the film above the debond crack was buckled as shown in Fig. 5.

Measured debond diameters taken from the Nomarski micrographs for various indentation loads in the range 2 to 30 N are shown in Fig. 6. The data closely follow the relation

$$a = kF^{1/3} \tag{2}$$

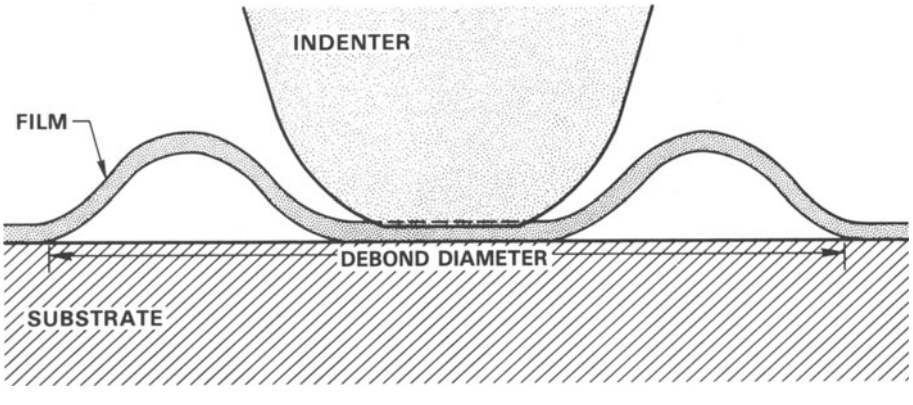

Fig. 5. Schematic of indentation-induced delamination at the interface of a thin film and substrate produced by a spherical indenter.

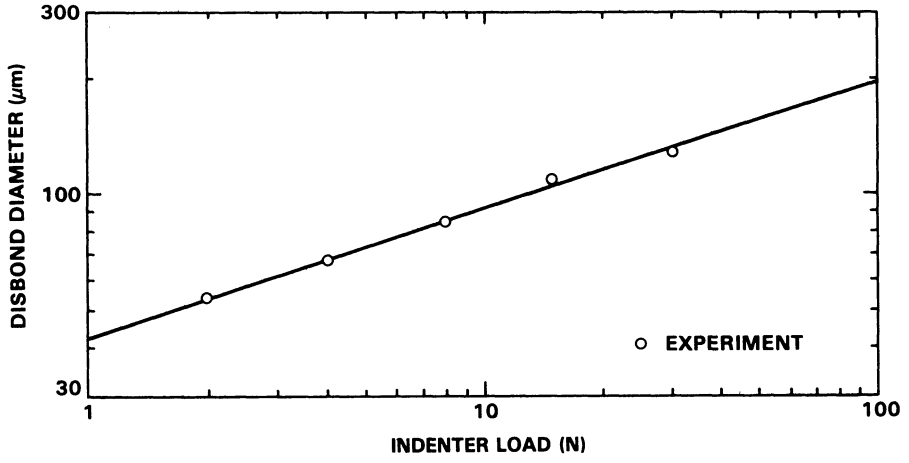

Fig. 6. Experimentally measured variation of the diameter of the disbond produced by the spherical indenter vs the load on the indenter. A line having a slope of 1/3 has been drawn through the experimentally measured points.

where a is the debond radius, F is the indentation force and k is a constant. The load range in Fig. 6 was limited at the lower end by the absence of crack initiation and at the upper end by permanent deformation of the tungsten carbide ball. In the gold/chrome/sapphire specimen, cracks did not initiate at the upper load of 30 N, indicating that the bond strength is considerably higher than in the gold/sapphire specimen. Larger indentation forces (and enhanced tendency for crack initiation) could be achieved by using an indenter with a larger diameter (see below).

Quantitative evaluation of debond resistance from the data in Fig. 6 requires fracture mechanics analysis to relate the debond radius to the indentation force and the debond fracture energy. In the present indentation/fracture configuration (Fig. 5), the spherical indenter leaves a permanent impression in the gold film, but the deformation of the indenter and substrate is purely elastic, provided the load does not exceed a critical value ($\approx$ 30 N for the 400 μm diameter ball). The plastic deformation of the film at the contact site generates local residual stresses which provide the driving force for delamination. The driving force is determined by the volume of film displaced by the indenter and, for a given volume, is not sensitive to indenter geometry. Results of a fracture mechanics analysis derived by Marshall and Evans [10] for the crack configuration of Fig. 5 are reproduced in Fig. 7, where the normalized crack length is plotted as a function of the crack driving force (i.e., the volume, V_0, of film displaced by the indenter) for various values of normalized residual deposition stress in the film. Comparison of the results in Fig. 6 with the analysis of Fig. 7 requires measurement of the normalized residual stress parameter, $\mathscr{R}$, and derivation of a relation between the indenter load and the displaced volume.

If residual deposition stresses in a film exceed a critial value, then spontaneous debonding should occur, initiating at the edge of the film. From a fracture mechanics analysis of such debonding, the critical residual stress can be expressed

$$\sigma_R = \left(\frac{2G_c E_f}{t}\right)^{1/2} \qquad (3)$$

where G_c is the fracture energy of the interface, E_f is the Young's modulus of the film, and t is the film thickness. Spontaneous debonding was never observed in the films used in this study even when a crack was initiated at the edge of the film with a razor blade. Therefore, Eq. (3) can be used to estimate an upper bound for the residual stress parameter,

$$\mathscr{R} = \frac{0.617(1 - \nu_f)\sigma_R^2 t}{E_f G_c} \quad . \tag{4}$$

With Poisson's ratio, $\nu_f = 0.41$ we obtain $\mathscr{R} < 0.73$. Therefore, the load/crack-length relation for indentation debonds is given by one of the curves in Fig. 7 for buckled films, with $\mathscr{R}$ between zero and 0.73. In this region

$$\mathscr{C} = B\mathscr{P}^{1/2} \tag{5}$$

where B is a constant with value between 1 (for $\mathscr{R} = 0$) and 2 (for $\mathscr{R} = 0.73$). Substituting for the normalized variables in Eq. (5) and solving for a, we derive

$$a = \left[\frac{B^2 E_f (1 - \nu_f)\gamma_f \beta_f t^2}{G_c}\right]^{1/4} V_0^{1/4} \tag{6}$$

where $\gamma_f = [1.22/(1 - \nu^2)]$, $\beta_f = [1/2\pi(1 - \nu)]$, and the subscript f refers to the film.

To determine the relationship between the volume displaced, V_0, and the indenter load, F, we assume a model of the form shown in Fig. 8. From optical interference measurements, a small plastic penetration, δ, of the indenter into the gold film was detected, but the responses of the indenter and the substrate were elastic. However, the penetration was small (< 20 nm) compared with the film thickness and the contact area.

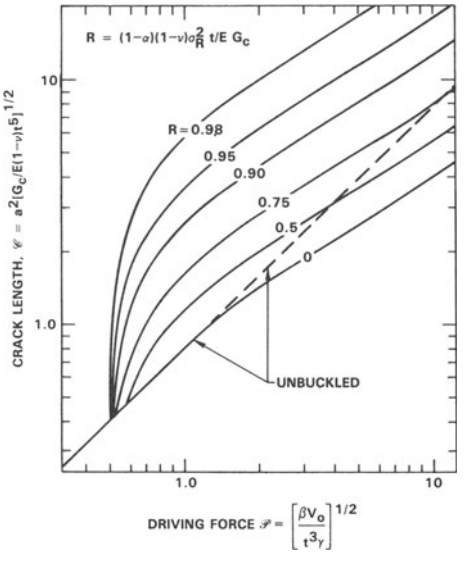

Fig. 7. Plot of normalized equilibrium crack length as a function of normalized indenter load, $\mathscr{P}$, for various levels of residual deposition stress. (After Marshall and Evans [10].)

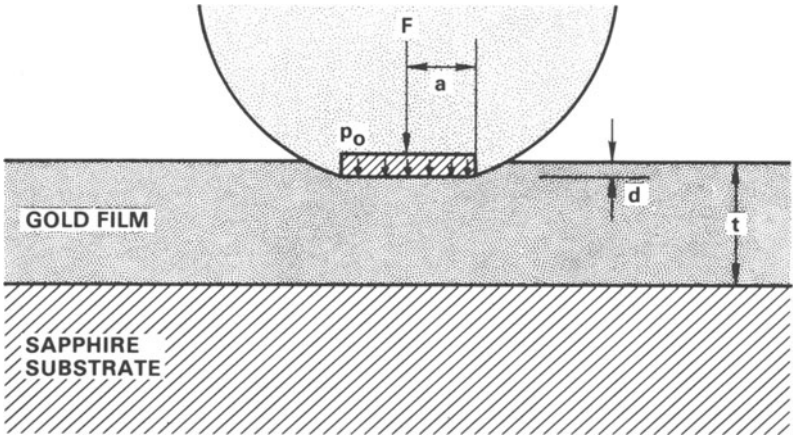

Fig. 8. Model for calculating the volume displaced by the spherical indenter.

Therefore the displaced volume is given approximately by

$$V_0 = \pi r^2 \delta \tag{7}$$

where the contact radius, r, is given by the Hertzian solution [14]

$$r = \left\{ \frac{3FR}{4E_s} \left[\left(1 - \nu_s^2\right) + \left(1 - \nu_i^2\right) \frac{E_s}{E_i} \right] \right\}^{1/3} \tag{8}$$

where R is the radius of the indenter and the subscripts s and i refer to the substrate and the indenter, respectively. The Hertzian contact assumption was confirmed experimentally by measuring the radius of the contact region on the chrome/gold film for a range of indenter loads that did not produce disbonds. The penetration of the indenter into the film was sufficiently small such that it was not possible to measure its variation with load accurately. Instead a nonlinear relation was assumed between the mean contact pressure, p_0, and the plastic strain, ε_p, in the film:

$$\frac{p_0}{\sigma_y} = (\varepsilon_p)^n = \left(\frac{\delta}{t}\right)^n \tag{9}$$

where σ_y is a constant. This relationship is expected to be nonlinear since the film is highly constrained in a small volume and the stress that is being imposed on the film ($p_0 \approx 5$ to 10 GPa) is orders of magnitude greater than the uniaxial yield stress of the gold. Rearranging Eq. (9), we deduce

$$\delta = t \left(\frac{p_0}{\sigma_y}\right)^{1/n} . \tag{10}$$

Note that $p_0 = (F/\pi r^2)$ so that, using Eqs. (7) and (8), the volume is

$$V_0 = \frac{\pi t}{(\pi \sigma_y)^{1/n}} \left(\frac{3R}{4E_s}\right) \left\{ \left[\left(1 - \nu_s^2\right) + \left(1 - \nu_i^2\right) \frac{E_s}{E_i} \right] \right\}^{2(1-1/n)} F^{2(1+1/2n)/3} . \tag{11}$$

From Eqs. (6) and (11), the relationship between the crack radius and the load is

$$a \propto F^{(1+1/2n)/6} \quad . \tag{12}$$

The value of n in the exponent can be calibrated from both Eq. (12) and the slope of the measured disbond diameter vs indenter load (Fig. 6). The slope of the line fitted through the experimental points in Fig. 6 is 1/3, giving n = 1/2. It is also necessary to estimate the constant, σ_y, used in Eq. (9) from measured data. For indentation at 30 N load (p_0 = 9 GPa), the depth of penetration of the indenter was estimated to be about 20 ± 5 nm using the interferometric measurements. These measurements, with t = 0.5 μm and Eq. (10), give σ_y = 40 ± 5 GPa.

Equations (6) and (9), with the calibration n = 1/2, provide an expression for the fracture energy G_c:

$$G_c = \frac{B^2 E_f (1 - \nu_f) \gamma_f \beta_f t^3}{\pi \sigma_y^2} \left\{ \frac{3R}{4E_s} \left[(1 - \nu_s^2) + (1 - \nu_i^2) \frac{E_s}{E_i} \right] \right\}^{-2/3} \left(\frac{F^{1/3}}{a} \right)^4 \tag{13}$$

where the subscripts f, s, and i refer to the film, substrate, and indenter, respectively. A value of $G_c = 3.3 \times 10^{-2}$ J/m^2 for the gold/sapphire interface was calculated from Eq. (13), assuming that the residual deposition stress is zero (i.e., B = 1) and using the measurement $(F^{1/3}/a) = 47 \times 10^3$ N$^{1/3}$/m from Fig. 6 with the following material constants and specimen dimensions: E_f = 81 GPa, E_s = 417 GPa, E_i = 616 Gpa, ν_f = 0.41, ν_s = 0.24, ν_i = 0.22, R = 200×10^{-6} m, t = 5×10^{-7} m, and σ_y = 40 GPa. With the upper bound estimate for the residual stress (i.e., B = 2), a value of $G_c = 1.4 \times 10^{-1}$ J/m^2 is obtained. This range of fracture energies of the gold film is comparable to that estimated for van der Waals forces (0.01 to 0.1 J/m^2). In comparison, values of G_c for some bulk materials are: $Al_2O_3 \approx 10$ J/m^2, MgO ≈ 3 J/m^2, and NaCl ≈ 0.6 J/m^2.

DISCUSSION

The SAM measurement technique provides a unique way to make precise quantitative nondestructive measurements of SAW velocities in small areas on a thin film/substrate system. We have shown both experimentally and theoretically that changes in the SAW velocities can be produced by changes in the compliance of the bond between the thin film and the substrate. We expect a correlation between the bond compliance and the bond fracture energy if the interfacial failure occurs by brittle fracture. To correlate bond compliance and fracture energy, we have explored the use of an indentation technique to measure bond fracture energy. The technique was used to measure the fracture energy of a gold film that was attached to a sapphire substrate by relatively weak van der Waals forces. However, in the more strongly adhered chrome/gold film, debonds could not be produced with the available range of contact parameters available (at indenter loads above about 30 Kg, the indenter tip deformed inelastically). A higher crack driving force with the same pressure at the indenter tip could be achieved by using a tip of larger radius. In future work we will take this approach to extend the indentation results to films with higher values of G_c. By making both acoustic and indentation measurements on the same film/substrate system, the correlation between the film/substrate bond compliance and its fracture energy can be established.

ACKNOWLEDGEMENT

Funded by the Rockwell Independent Research and Development Program.

REFERENCES

1. K. L. Mittal, "Adhesion measurements of thin films," Electrocomp. Sci. Technol. vol. 3, pp. 21-42, 1976.

2. K. L. Mittal, "A critical appraisal of the methods for measuring adhesion of electrodeposited coatings," in Properties of Electrodeposits: Their Measurement and Significance, ed. R. Sard, H. Leidheiser, Jr., and F. Ogburn, Chapter 17, pp. 273-306, The Electrochemical Society, Princeton, New Jersey, 1975.

3. C. Weaver, "Adhesion of thin films," J. Vac. Sci. Technol., vol. 12, pp. 18-25, 1975.

4. D. S. Campbell, "Mechanical properties of thin films," in Handbook of Thin Film Technology, ed. L. I. Maissel and R. Glang, Chapter 12, McGraw Hill Book Company, New York, 1970.

5. J. Kushibiki and N. Chubachi, "Material characterization by line-focus-beam acoustic microscope," IEEE Trans Sonics Ultrason., vol. SU-32, pp. 189-212, 1985.

6. R.C. Addison, Jr., M. Somekh, and G.A.D. Briggs, "Techniques For The Characterization Of Film Adhesion," 1986 Ultrasonics Symposium Proceedings, pp. 775-782, IEEE, 1987. IEEE cat # 86CH2375-4

7. A. Atalar, "An angular spectrum approach to contrast in the reflection acoustic microscope," J. Appl. Phys., vol. 49, pp. 5130-5139, 1978.

8. R. D. Weglein, "A model for predicting acoustic material signatures," Appl. Phys. Lett., vol. 34, pp. 179-181, 1979.

9. S. S. Chiang, D. B. Marshall, and A. G. Evans, "A Simple Method For Adhesion Measurements," in Surfaces and Interfaces in Ceramic and Ceramic-Metal Systems, ed. J. A. Pask and A. G. Evans, vol. 14, pp. 603-617, Plenum, New York, 1981.

10. D. B. Marshall and A. G. Evans, "Measurement of adherence of residually stressed thin films by indentation. I. Mechanics of interface delamination," J. Appl. Phys., vol. 56, pp. 2632-2638, 1984.

11. R. C. Bray, "Acoustic and photoacoustic microscopy," Ph.D. Thesis, Stanford University, 1981.

12. R. B. Thompson and C. J. Fiedler, "The effects of crack closure on ultrasonic scattering measurements," in Review of Progress in QUANTITATIVE NONDESTRUCTIVE EVALUATION v.3, ed. D. O. Thompson and D.E. Chimenti, pp. 207-215, Plenum Press, N.Y., 1984.

13. M. Punjani and L. J. Bond, "Scattering of plane waves by a partially closed crack," in Review of Progress in QUANTITATIVE NONDESTRUCTIVE EVALUATION v.5, ed. D.O. Thompson and D.E. Chimenti, pp. 61-71, Plenum Press, N.Y., 1986.

14. B. R. Lawn and T. R. Wilshaw, "Indentation Fracture: Principles And Applications," J. Mater. Sci., vol. 10, pp. 1049-1081, 1975.